

UMR - 37

PROGRESS REPORT NO. 9

AAF CONTRACT W33-038 ac 2100

PERIOD 9

1 November, 1949, to 1 January, 1950

TABLE OF CONTENTS

	Page No.
I. List of Figures	3
II. Summary of Work Conducted During the Period 1 November 1949 to 1 January 1950	4
III. Progress	
Blowoff Velocities of Flame Holders and Pressure and Temperature Effects on Combustion Processes.	5
Combustion Chamber Design	20
Flow Associated With the V-Flame	23
Detonation	24
Blowdown Equipment	26
Experimental Techniques and Instrumentation	31
IV. Program Planned for Period 10 1 January 1950 to 1 March 1950	33
V. Activities Visited	34
VI. Bibliography	35
VII. Distribution	36

LIST OF FIGURES

<u>Figure Number</u>		<u>Page</u>
1	Mass Velocity at Blowoff vs. Absolute Pressure (3/8" diameter nozzle - 1/16" diameter sphere - rich mixtures)	8
2	Mass Velocity at Blowoff vs. Absolute Pressure (3/8" diameter nozzle - 1/16" diameter sphere - lean mixtures)	9
3	Mass Velocity at Blowoff vs. Absolute Pressure (3/8" diameter nozzle - 0.19" diameter sphere - rich mixtures)	10
4	Mass Velocity at Blowoff vs. Absolute Pressure (3/8" diameter nozzle - 0.19" diameter sphere - lean mixtures)	11
5	Effect of Pressure on Mass Velocity at Blowoff (3/8" diameter nozzle - 1/16" diameter sphere)	12
6	Effect of Pressure on Mass Velocity at Blowoff (3/8" diameter nozzle - 0.19" diameter sphere)	13
7	Fuel-air Ratio vs. Jet Velocity at Various Pressures (3/8" diameter nozzle - 1/16" diameter sphere)	14
8	Fuel-air Ratio vs. Jet Velocity at Various Pressures (3/8" diameter nozzle - 3/32" diameter sphere)	15
9	Fuel-air Ratio vs. Jet Velocity at Various Pressures (3/8" diameter nozzle - 0.125 diameter sphere)	16
10	Fuel-air Ratio vs. Jet Velocity at Various Pressures (3/8" diameter nozzle - 0.19 diameter sphere)	17
11	Reynolds Number at Maximum Blowoff Velocity vs. Spherical Flame Holder Diameter for Various Pressures	18
12	Fuel-air Ratio vs. $\frac{1}{\text{Reynolds Number}}$ at Maximum Blowoff Velocity at Various Pressures	19
13	Apparatus Used for Tests of Burning Velocity	21
14	Blowoff Velocity Comparison Graph	22
15	Perspective View of Blowdown System	27
16	Cutaway of Heat Exchanger	28
17	Preliminary Heating Run Data	29
18	Blowoff Velocity Test Section	30
19	Schematic of Photoflash Unit	32

II. SUMMARY OF WORK CONDUCTED DURING THE PERIOD

Blowoff Velocities of Flame Holders and Pressure and Temperature Effects on Combustion

Blowoff data for 1/16" and 0.19" diameter spherical flame holders were obtained in a 3/8" diameter jet for fuel-air ratios at pressures from 0.4 atmosphere to 1 atmosphere. These data, together with data previously obtained for 3/32" and 1/8" diameter spherical flame holders are presented in various graphs. The data indicate that reduced pressures have a decidedly adverse effect on stability limits of spherical flame holders.

Combustion Chamber Design

Four-inch Combustion Chamber - A new fuel-injection nozzle design for use in the four-inch combustion chamber has been designed and constructed in an attempt to correlate rough burning and combustion efficiency with the relative positions of fuel injection and flame holding.

High Intensity Combustion - Experiments have indicated that radiant energy can be used to hold flame in a burner, permitting higher mass flows of fuel-air mixtures than are possible with conventional flame holders.

Flow Associated with the V-flame

An external memorandum has been written on "Resonance of a V-flame in a Parallel-walled Combustion Chamber." This report will be distributed.

Detonation

Detonation studies were continued and it was found that the spark source was not fast enough to stop the high velocity shock waves and the test section windows were not clear enough to obtain good shadowgraphs.

Blowdown Equipment

Heat Exchanger - Several heating runs have been made with the blowdown system and general operation data obtained. Several operational difficulties have been corrected at this point. A test section has been constructed to determine the effect of mixture temperature upon flame holding.

Hypersonic Flow Studies - A Mach 6 nozzle has been designed and is in the process of being constructed.

Experimental Techniques and Instrumentation

Interferometer - Deliveries are being made on previously contracted sub-assemblies. Additional contracts are being let as drawings are completed.

Shadowgraph Equipment - Construction of a photoflash unit for the laboratory has been completed.

III. PROGRESS

Blowoff Velocities of Flame Holders and Pressure and Temperature Effects on Combustion

Part 1 of the program outlined in Progress Report No. 8 (1a) was completed and the data are presented herein. Data obtained on parts 2 and 3 are as yet incomplete and will be presented in a later report.

The data obtained for part 1 of the program extended the range of spherical flame holder diameters tested for flame stability.

In period 8 the flame stability limits of a 3/32" and 1/8" diameter spherical flame holders were obtained under varying degrees of vacuum. In this period, similar tests were made using 1/16" and 0.19" diameter spheres. Data were obtained in a 3/8" diameter jet under pressures of 1 atmosphere to 0.4 atmosphere for fuel-air ratios $\left(\frac{\text{lbs. C}_3\text{H}_8}{\text{lbs. air}}\right)$ of 0.06, 0.0637, 0.070, 0.075, 0.080, 0.085, 0.090, 0.095, and 0.100. The experimental technique and the system described in Progress Report No. 8 (2a, 3a) were used to obtain these data.

The experimental data obtained for these spheres had approximately the same scatter as the data previously presented, therefore, only graphical summaries of the data are presented here. Figures 1 and 2 show plots of mass velocity (i.e., lbs/sec-ft² nozzle area, or linear velocity X density) at blowoff for variable pressures and fuel-air ratios, using a 1/16" sphere for a flame holder. Absolute pressure and mass velocity were the two variables measured instantaneously while fuel-air ratio was held constant during each run. Figures 3 and 4 show the same plots except that a 0.19" spherical flame holder is used. Because of overlapping of plotted data, separate graphs have been drawn for the rich and lean mixtures. These figures may be compared with those of the previous report (4a).

Figures 5 and 6 are constructed from the data of Figures 1 through 4. Figures 5 and 6 are plots of propane mass velocity at blowoff vs. air mass velocity at blowoff for the 1/16" and 0.19" diameter spherical flame holders respectively. Parameters of 750, 600, 450, and 300 mm. H_g absolute pressure are shown. These figures may be compared to the data previously presented (5a) for the 3/32" and 1/8" diameter spherical flame holders and also to the data for the four flame holders in a 1" diameter jet at atmospheric pressure (6a).

It is a characteristic of this type of plot that a straight line through the origin is a line of constant fuel-air ratio. For the flame holder, jet, and pressure used, any point in the area inside of a given curve represents conditions in which it is possible to maintain a stable flame, while a point outside the curve represents conditions in which it is not possible to maintain a stable flame.

The data obtained during this phase of the investigation indicate the large decrease in stability limits due to the reduction of pressure. The relative

effects of fuel-air ratio and flame holder size appear small when compared to the effect of reduced pressure. While it might be hypothesized that a different system would give different numerical values of the mass blowoff velocity, it is believed that the relative effects of pressure would not change a great deal for the fuel used.

The data shown in Figures 1, 2, 3, and 4 of this report and in Figures 8, 9, 10, and 11 of the previous report were used to prepare Table I below:

TABLE I

3/8" Diameter Jet

Spherical Flame Holder Diameter (inches)	Fuel-air Ratio (lbs. C ₃ H ₈ /lb. air)	
	0.100, 0.095 0.090, 0.085	0.080, 0.075, 0.070, 0.0637, 0.060
	Blowoff Mass Velocity at 0.5 atmosphere Blowoff Mass Velocity at 1.0 atmosphere	
1/16	0.102 to 0.138	0.090 to 0.107
3/32	0.210 to 0.190	0.173 to 0.120
1/8	0.270 to 0.210	0.193 to 0.133
0.190	0.300 to 0.220	0.232 to 0.235

It is seen that over a range of flame holder diameters from 1/16" to 3/16" and for fuel-air ratios varying from 0.060 to 0.100, the blowoff mass velocity at 1/2 atmosphere averages about 1/5 of the blowoff mass velocity at 1 atmosphere.

Since the thrust per unit area of a fixed geometry jet engine is directly proportional to this mass velocity, it would follow that the thrust per unit area would be considerably more reduced at high altitudes than the value predicted by the lower ambient density at these conditions.

The data listed in the program outline of the previous progress report (1a) are presented in graphical form in this report. The data obtained during this period and the preceding period has been cross plotted to obtain graphs of fuel-air ratio versus linear jet velocity with parameters of absolute pressure. Figures 7, 8, 9, and 10 are plotted for 1/16", 3/32", and 1/8", and 0.19 inch diameter spherical flame holders, respectively. It should be recognized that the linear velocities thus plotted were not obtained from the smoothed out curves of mass velocity vs pressure, but were obtained directly from the experimental data.

Figure 11 is a plot of spherical flame holder diameter vs. the Reynolds number at maximum mass blowoff velocities (i.e., the mass velocity corresponding to the peaks of the curves of Figures 5 and 6 of this report and Figures 12, 13, and 14 of the previous report (5a, 6a).

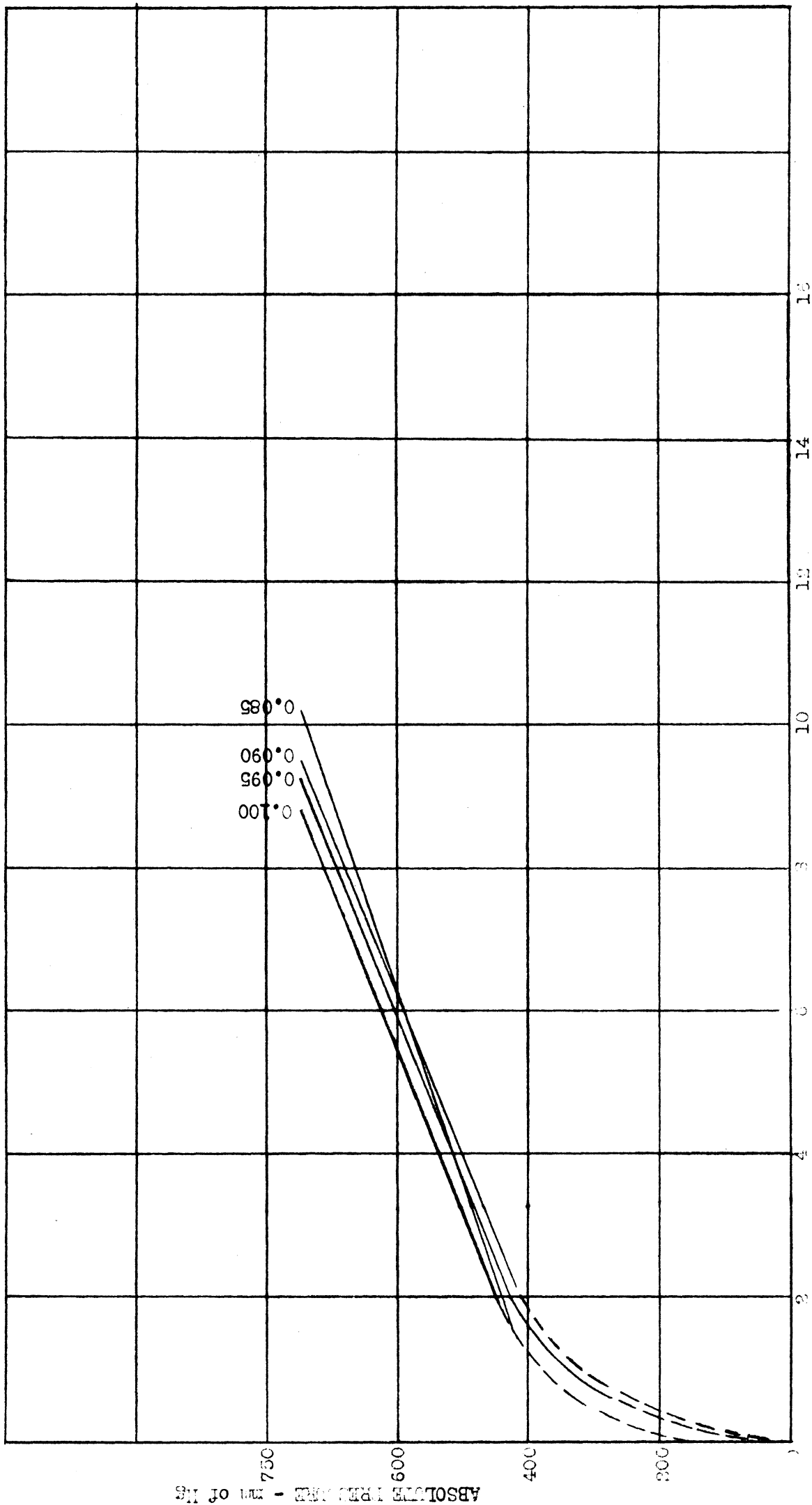
The length dimension used in calculating the Reynolds number was the spherical flame holder diameter. It is interesting to note that the lines of constant

pressure shown on this plot tend to intersect at a very low Reynolds number and a sphere diameter of about 0.04 inches. It would indicate that there is a minimum sphere diameter below which the flame could not be stabilized for this particular system. To establish this point it would be necessary to test a spherical flame holder less than 0.04 inches diameter in the same jet. However, as may be seen from Figure 11, there is some disagreement between the data obtained in a 1" jet and that obtained in a 3/8" jet for atmospheric pressure which must be reconciled before definite conclusions are drawn.

Figure 12 is a plot of fuel-air ratio vs. the reciprocal of the square root of the Reynolds number at maximum mass blowoff velocities. It had previously been established that this type of plot gave a straight line for the data obtained in the 1" jet at atmospheric pressure. These data are shown in Figure 12 together with the data obtained in the 3/8" jet under reduced pressures for the same flame holder diameters. The data obtained in the 3/8" jet gives a straight line for the three larger sphere sizes, but the 1/16" diameter sphere apparently reaches its maximum mass velocity at a leaner fuel-air ratio than would be expected from a straight line extrapolation of the larger flame holder sizes.

The inconsistency between jet sizes for 1 atmosphere pressure is also evident from this plot. An attempt is currently being made to explain these discrepancies.

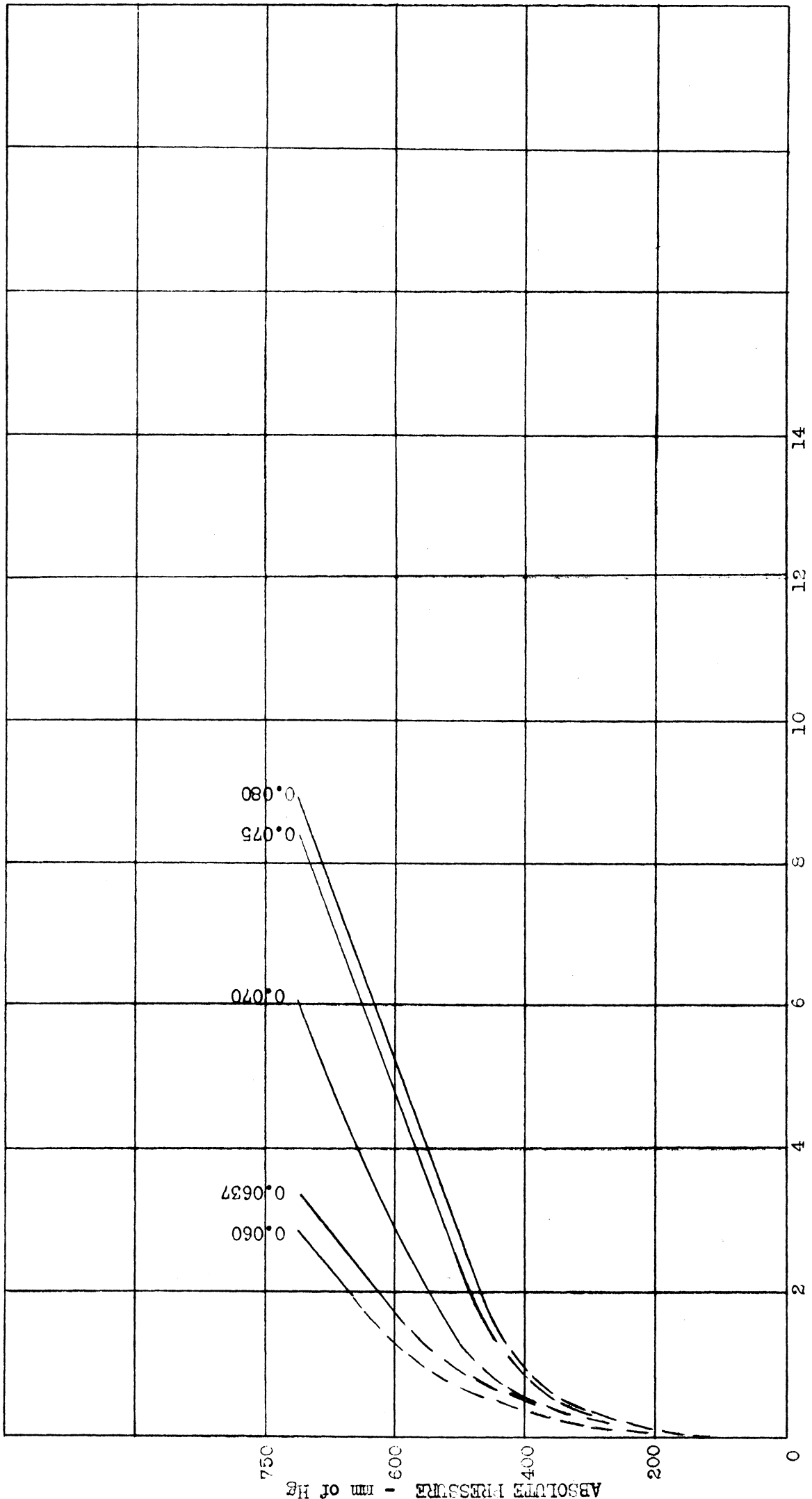
Figure 1
 MASS VELOCITY AT BLOWOFF
 VS.
 ABSOLUTE PRESSURE
 3/8" DIAMETER NOZZLE
 1/16" DIAMETER SPHERE



MASS VELOCITY AT BLOWOFF (LBM/SEC - FT.)

ABSOLUTE PRESSURE - mm of Hg

Figure 2
MASS VELOCITY AT BLOWOFF VS. ABSOLUTE PRESSURE
3/8" DIAMETER NOZZLE
1/16" DIAMETER SPHERE



MASS VELOCITY AT BLOWOFF (LBM/SEC - 5.0 FT. OF NOZZLE AREA)

Figure 3

MASS VELOCITY AT BLOWOFF
VS.
ABSOLUTE PRESSURE
3/8" DIAMETER NOZZLE
0.19" DIAMETER SPHERE

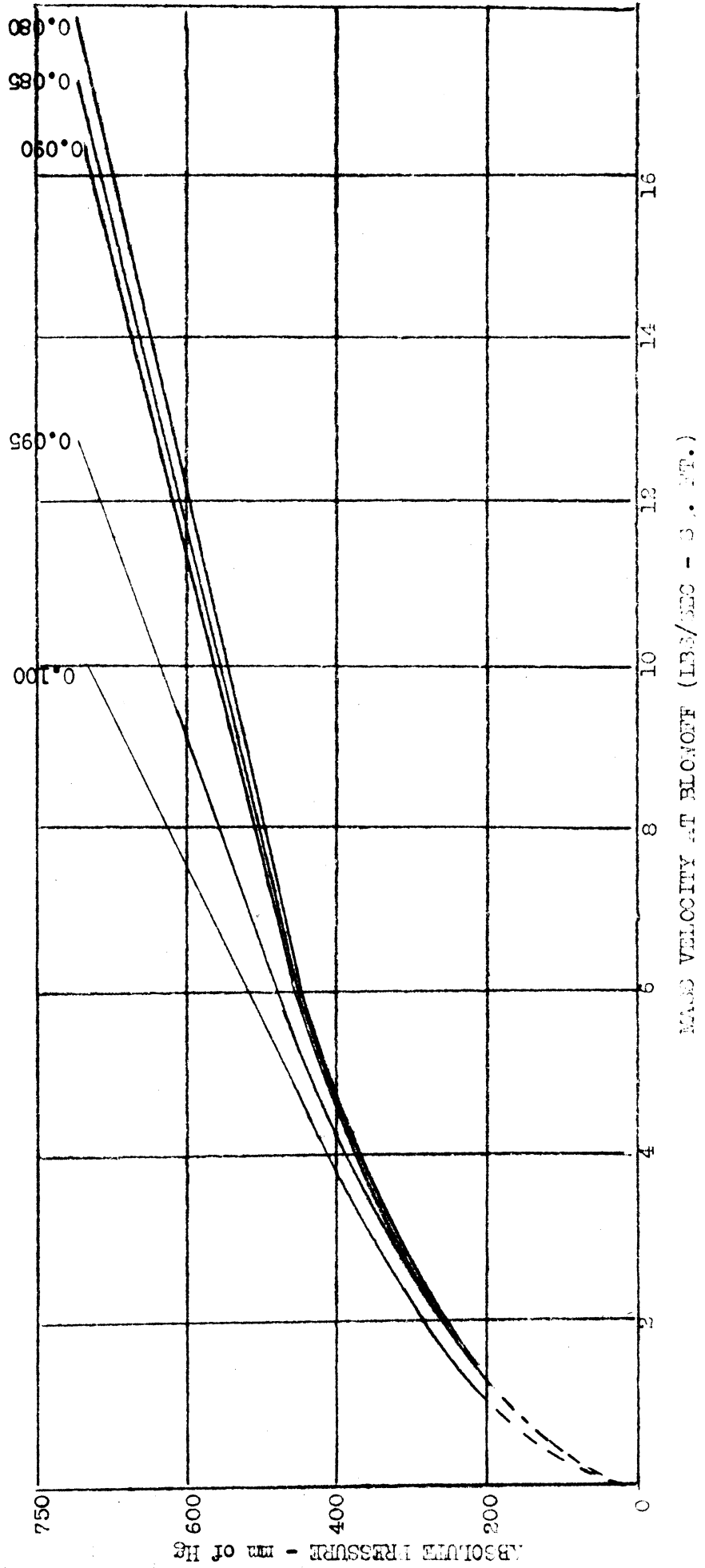


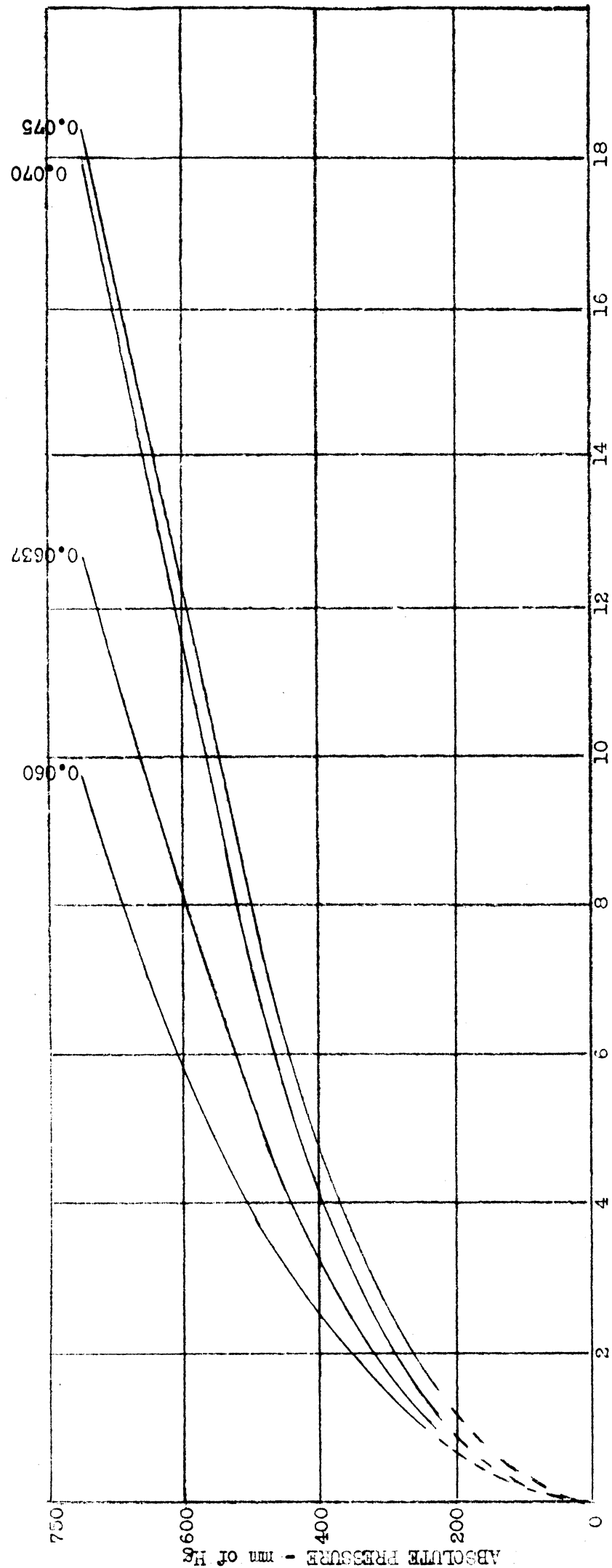
Figure 4

MASS VELOCITY AT BLOWOFF

V_b.

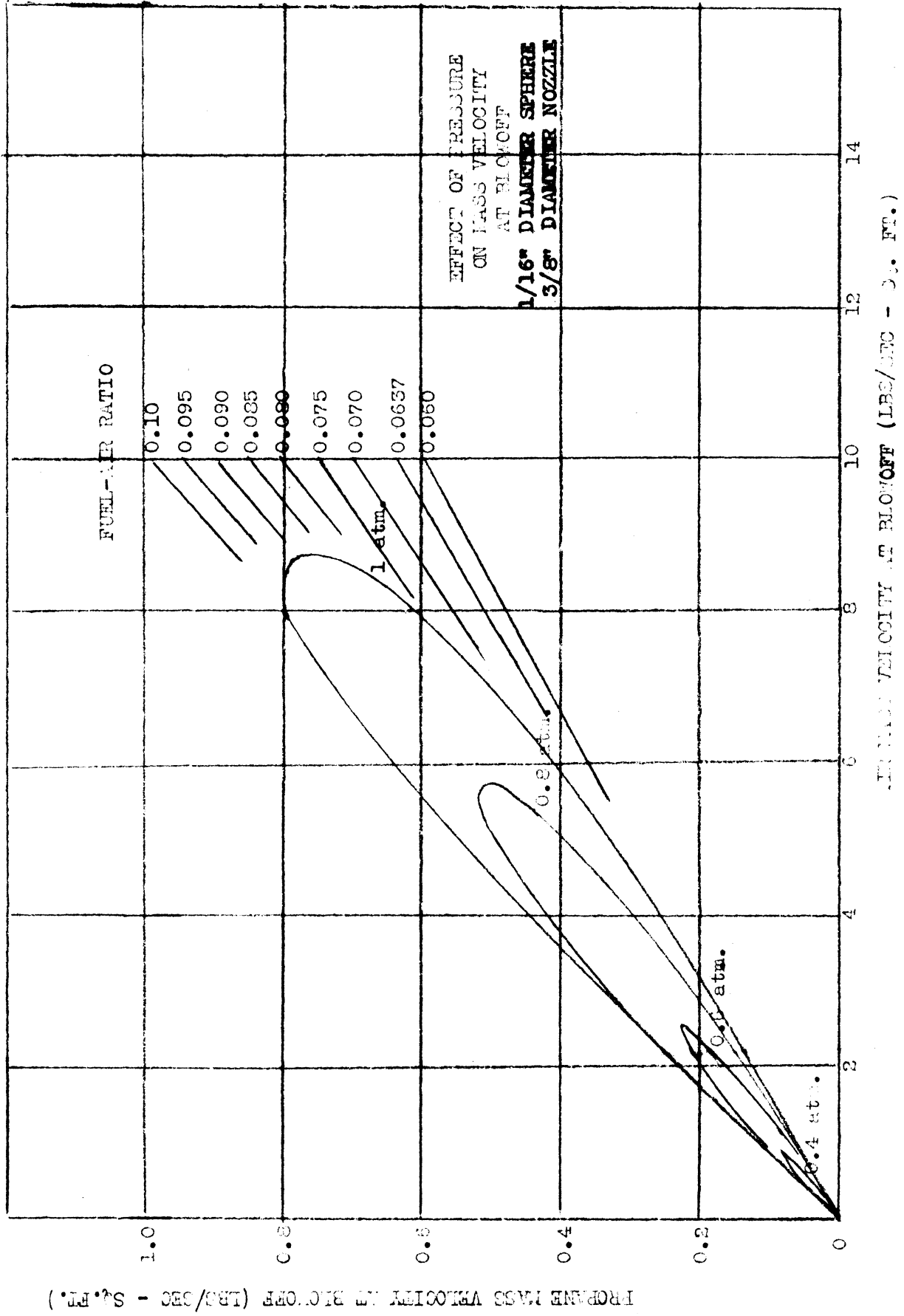
ABSOLUTE PRESSURE

3/8" DIAMETER NOZZLE
0.19" DIAMETER SPHERE



MASS VELOCITY AT BLOWOFF (LBS/SEC - SQ. FT.)

Figure 5



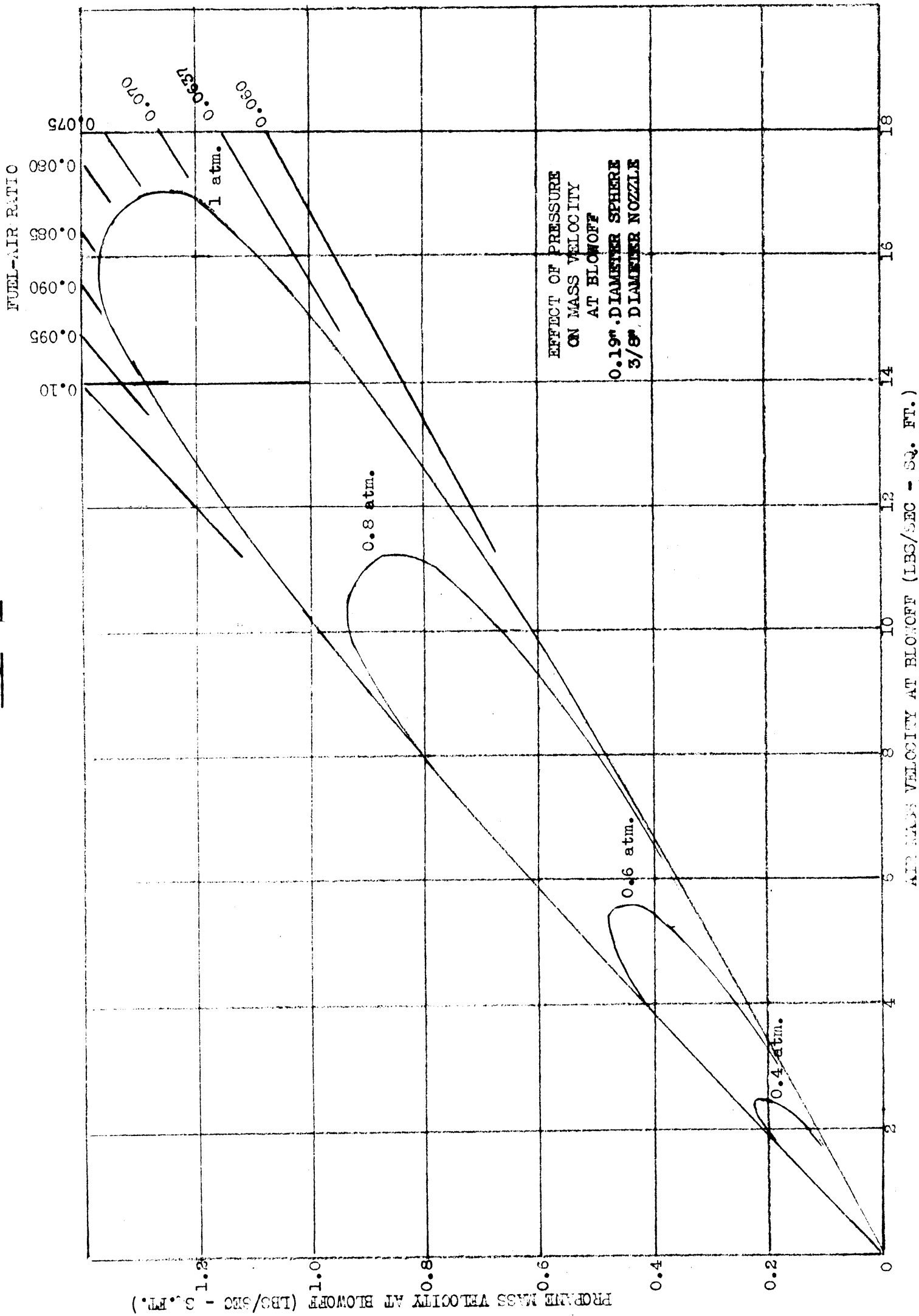


Figure 6

Figure 7

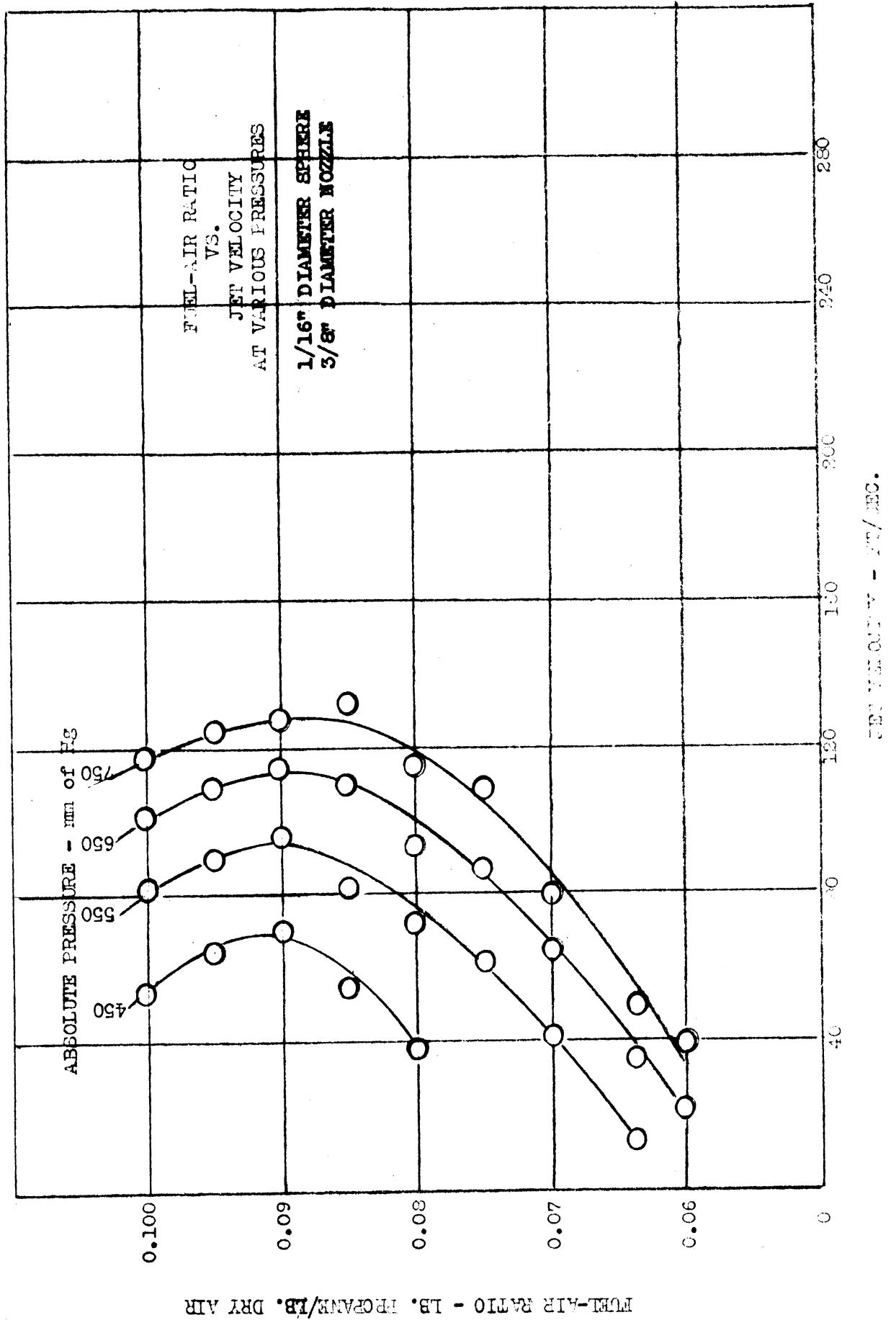


Figure 8

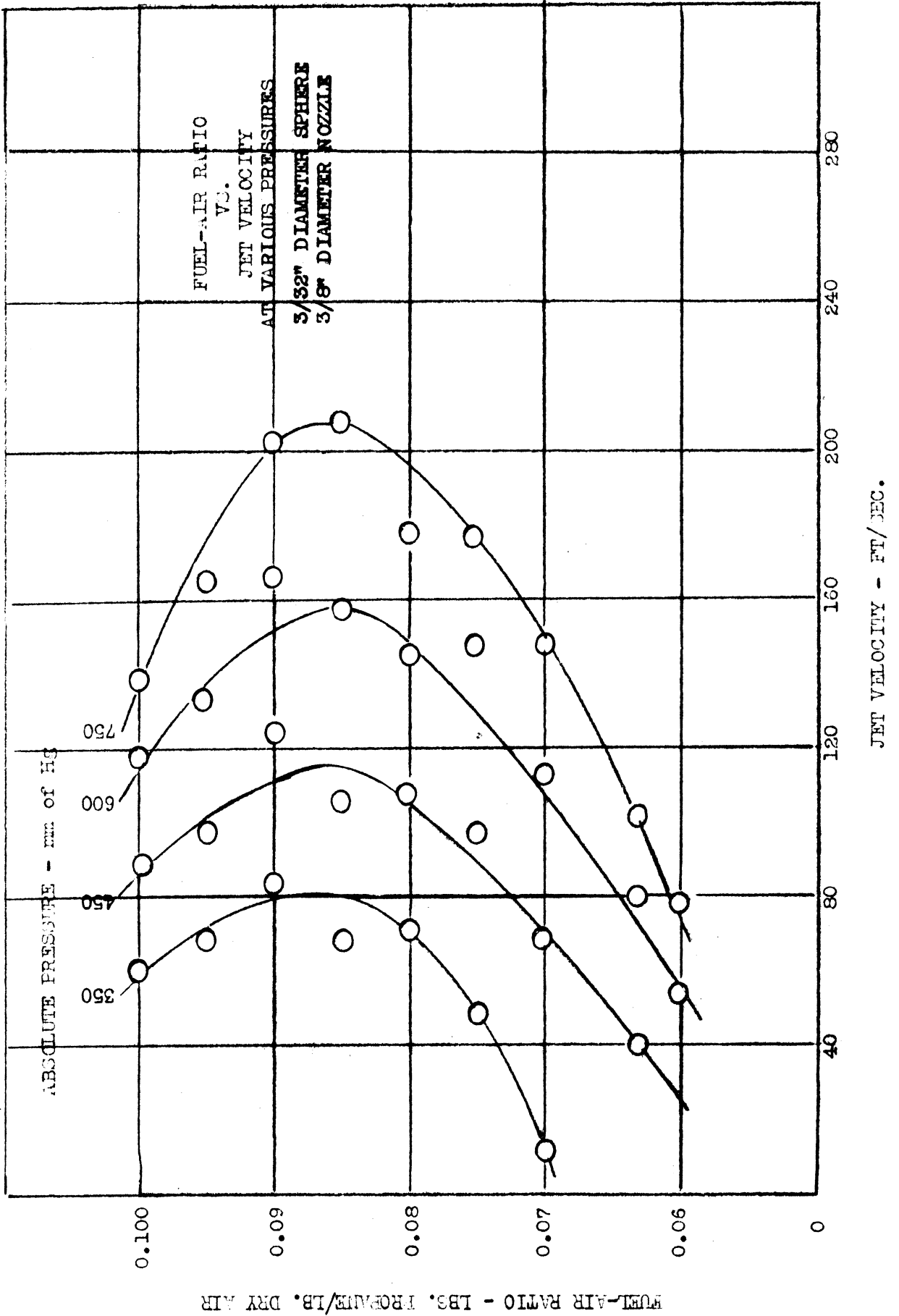


Figure 9

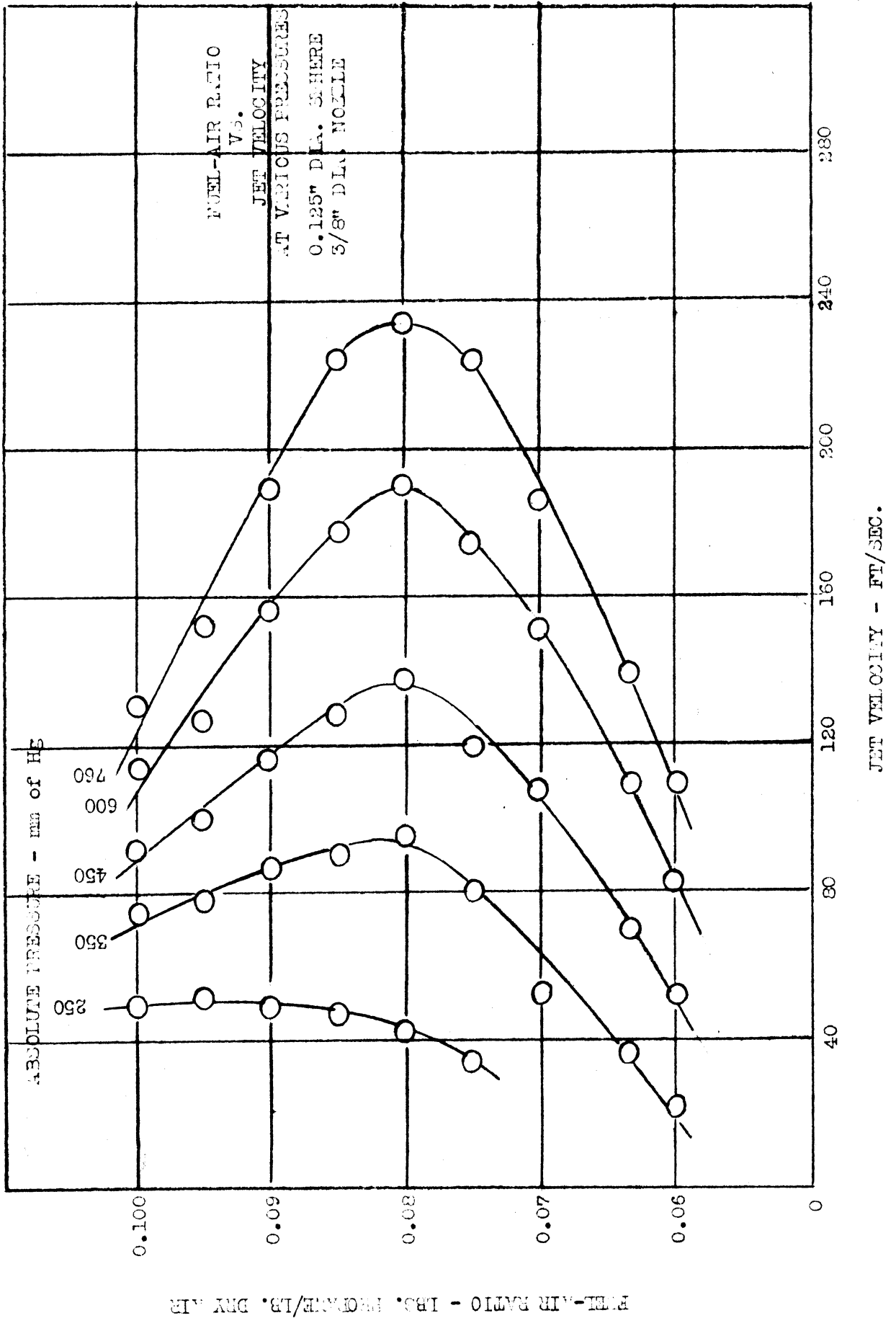
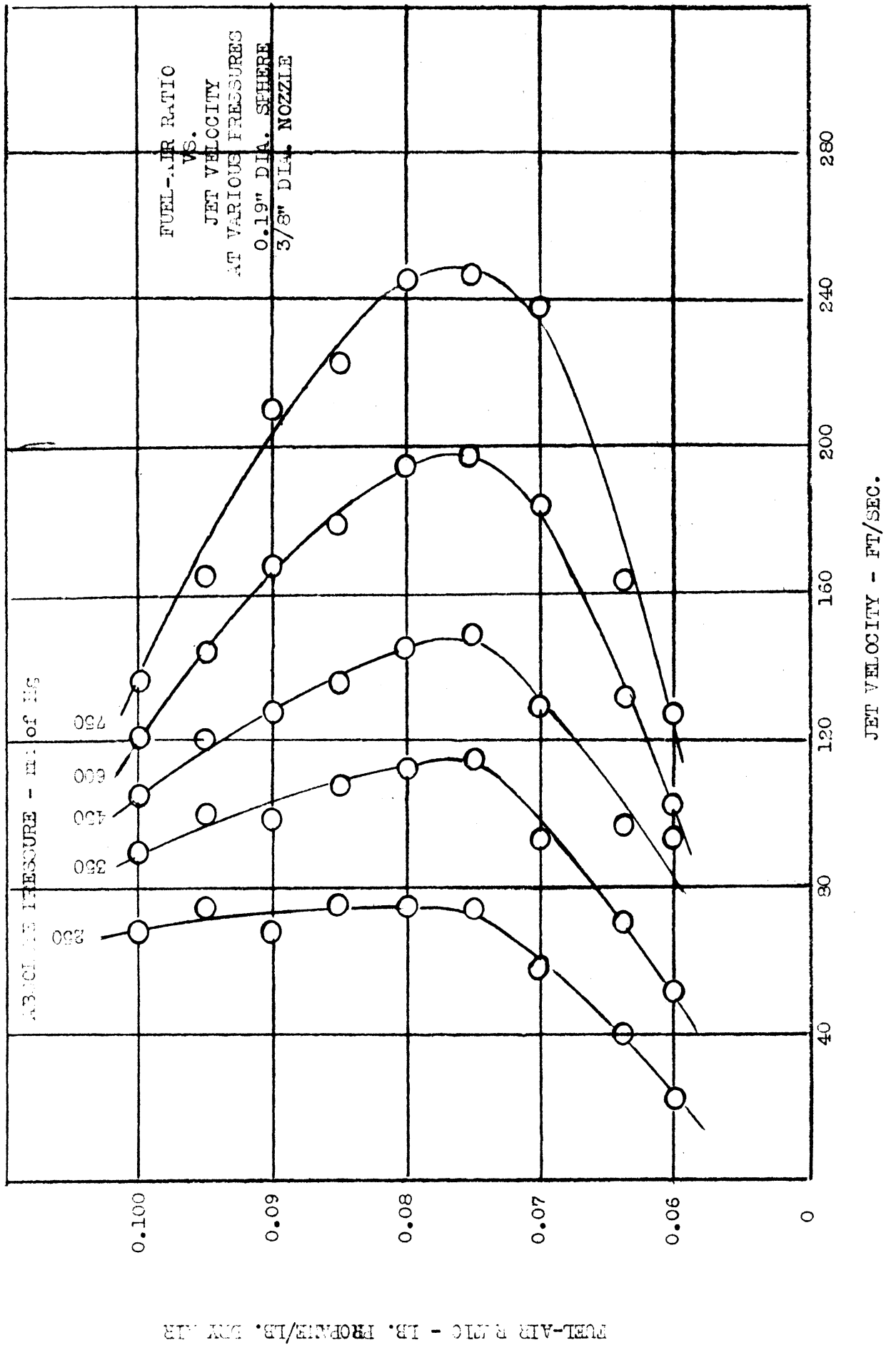
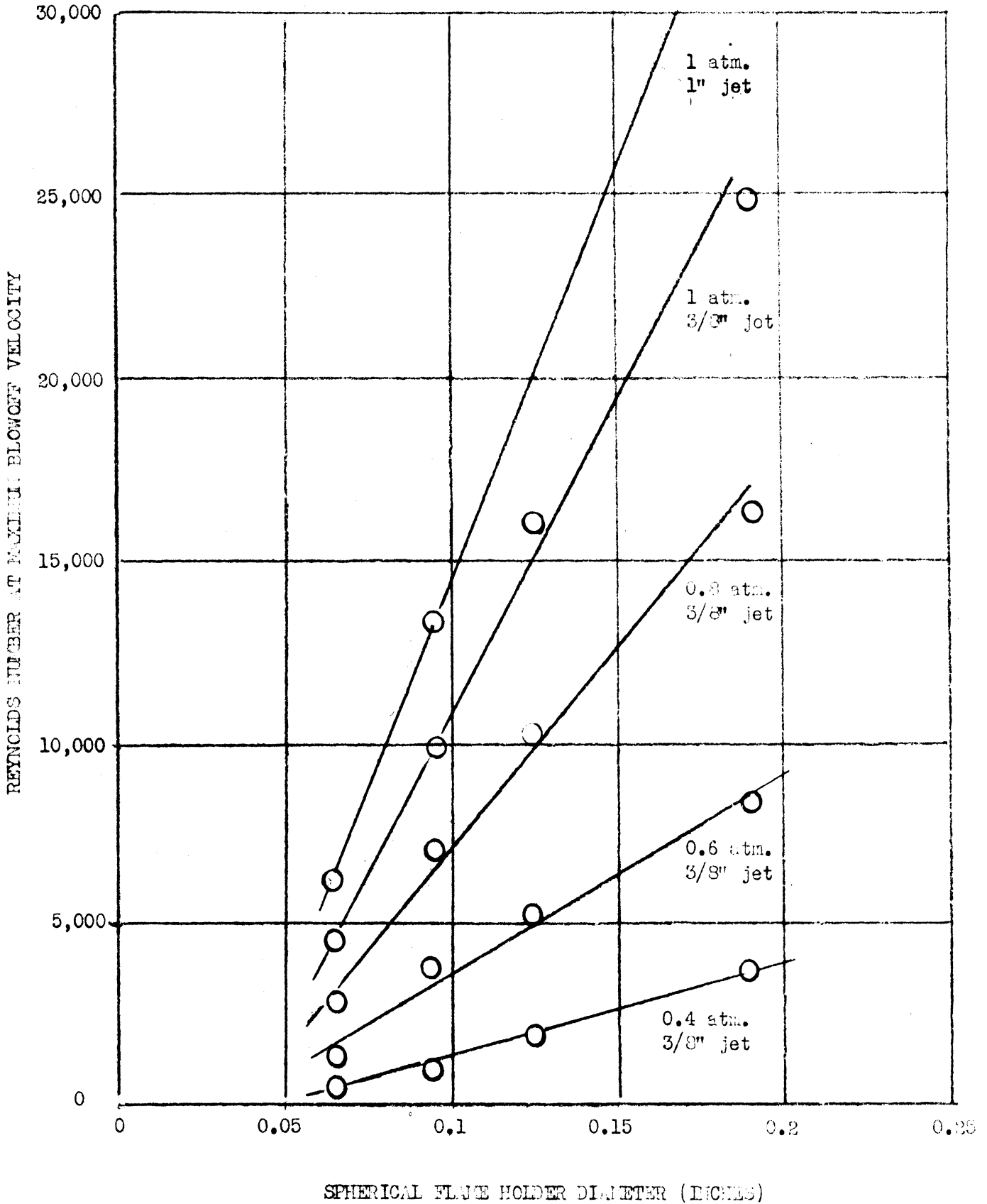


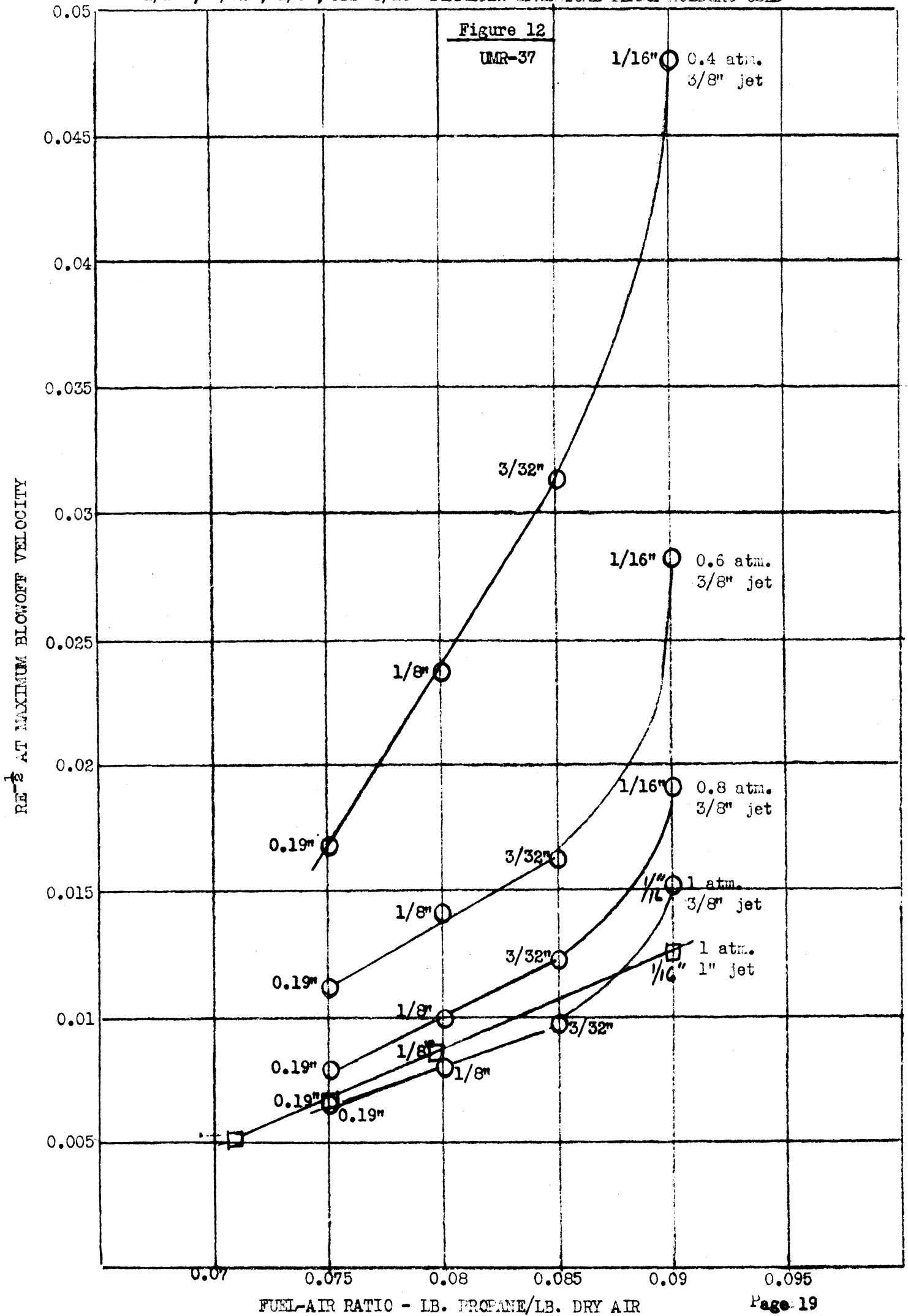
Figure 10



REYNOLDS NUMBER AT MAXIMUM BLOWOFF VELOCITY
VS.
SPHERICAL FLAME HOLDER DIAMETER FOR VARIOUS PRESSURES



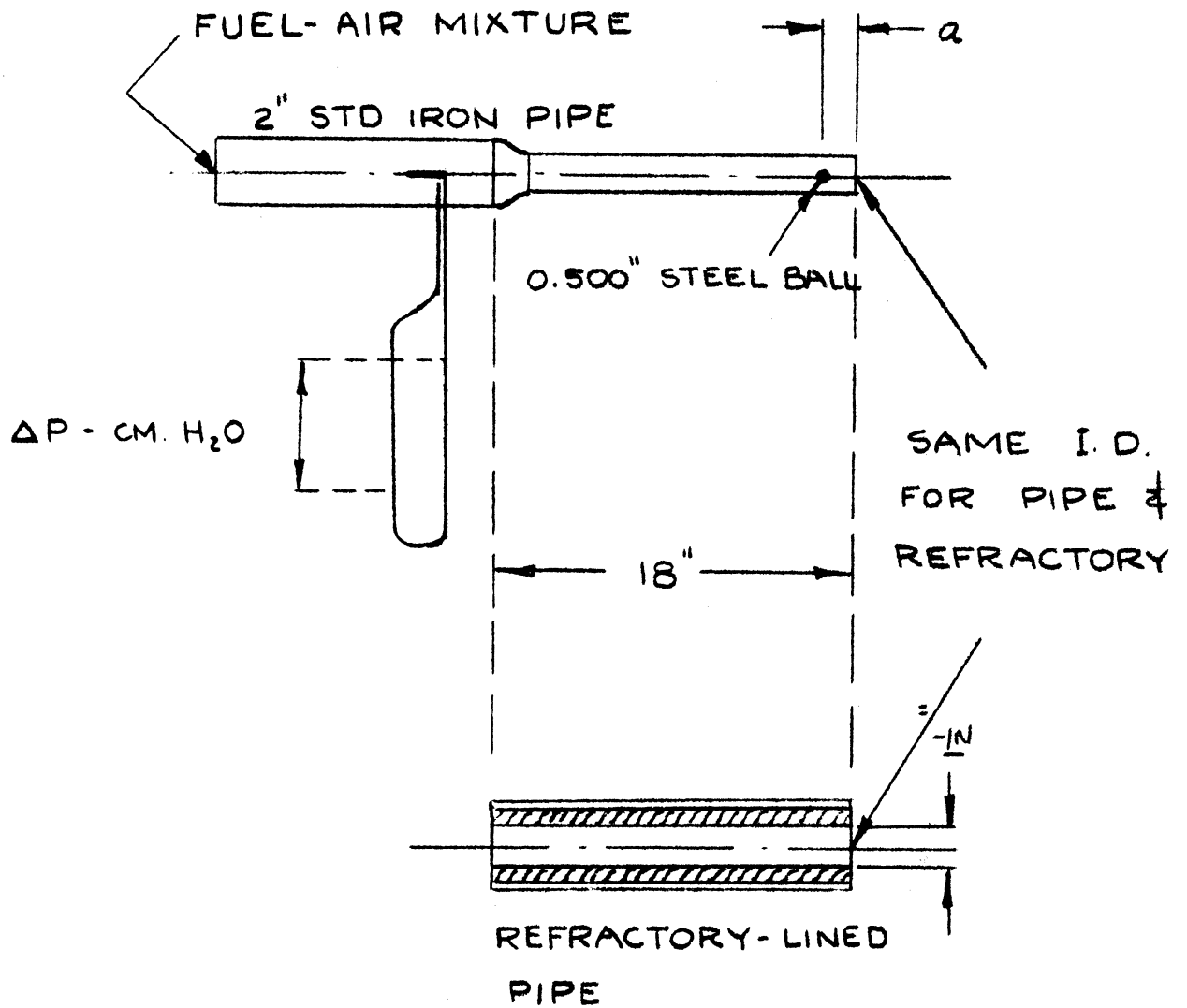
FUEL AIR RATIO VS. $RE^{-\frac{1}{2}}$ AT MAXIMUM BLOWOFF VELOCITY AT VARIOUS PRESSURES
 1/16", 3/32", 1/8", AND 3/16" DIAMETER SPHERICAL FLAME HOLDERS USED



Combustion Chamber Design

Four-inch Combustion Chamber - Previous work has indicated that the position of the fuel injection nozzle relative to the flame holder plays an important part in controlling the roughness of burning in the combustion chamber. It also appears likely that the relative position of the nozzle to the flame holder would have some effect upon combustion efficiency. With the fuel injection system used in past tests it was impossible to vary the nozzle position in other than small steps; each step required the removal of the nozzle and its re-assembly in the new position. A new nozzle injection section has been designed which allows continuous movement of the nozzle over an eight-inch range. Additional sections can further alter the nozzle flame holder relative positions. This new nozzle will be used in conjunction with the funnel-type flame holder, as discussed in Progress Report No. 8.

High Intensity Combustion - Experiments conducted recently indicate that radiant energy can be used to hold the flame in a burner. Two burners of the same internal diameters were used in the tests: one was a length of standard, iron pipe with a spherical flame holder which was moved upstream and downstream during the test; the other was a length of pipe lined with a high melting point refractory, but which had no conventional flame holder (see Figure 13). The refractory-lined pipe was able to hold the flame at considerably higher inlet mixture velocities than the unlined iron pipe. During the process of burning at maximum mixture flows, the inside of the refractory-lined pipe approached a white heat over a length of several inches. While factors other than the radiant energy (roughness, porosity, etc.) may be active in the flame holding process, it is felt that the results could not be duplicated on a basis of roughness and porosity alone, but that the radiant energy transmitted back to the mixture plays an important part in the rate of combustion.



APPARATUS USED FOR TESTS
OF BURNING VELOCITY

Figure 13

BLOWOFF VELOCITY COMPARISON

MAX. AIR-FUEL FLOW AVAILABLE AT TIME OF TESTS

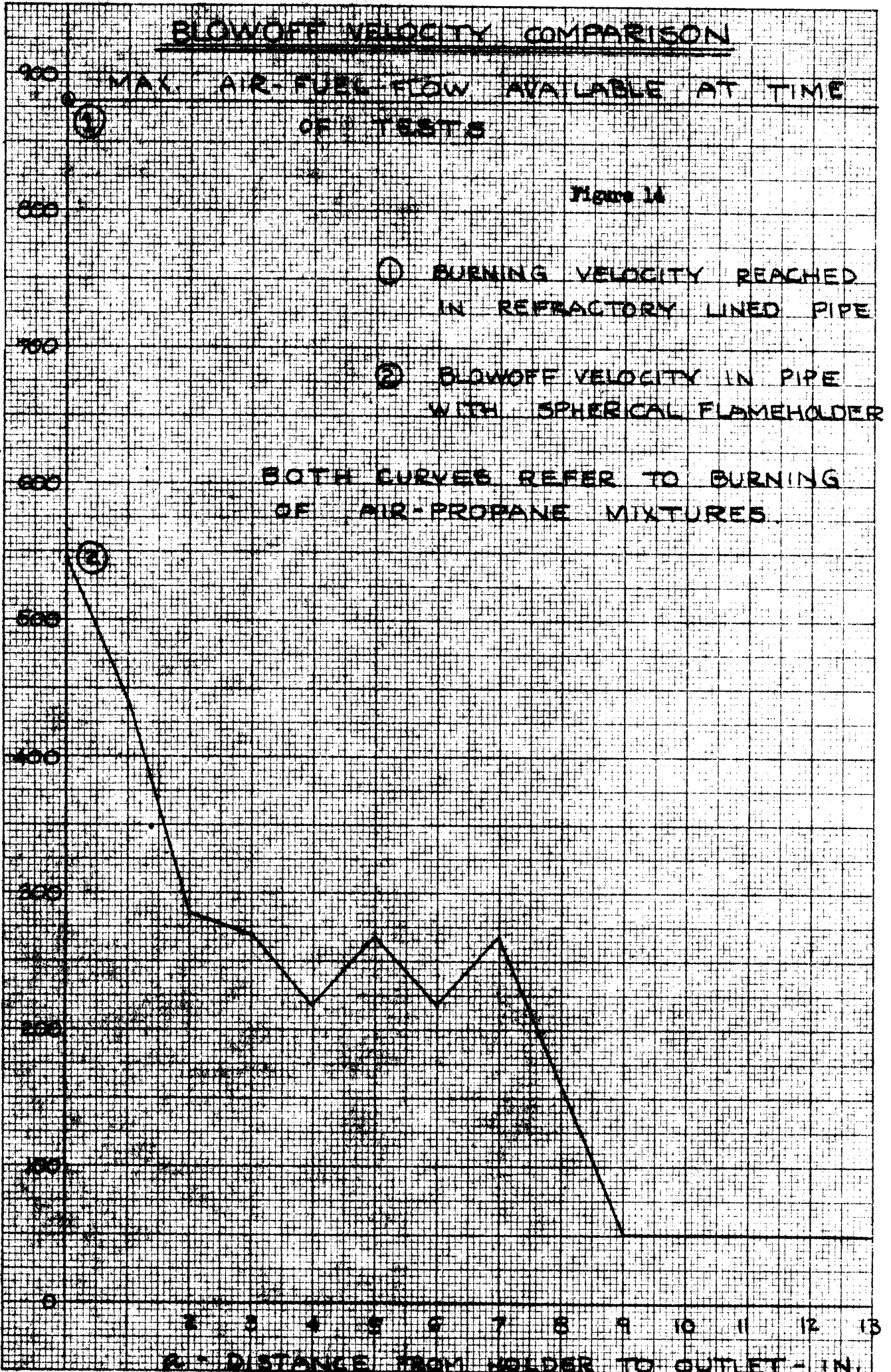
Figure 14

① BURNING VELOCITY REACHED IN REFRACTORY LINED PIPE

② BLOWOFF VELOCITY IN PIPE WITH SPHERICAL FLAMEHOLDER

BOTH CURVES REFER TO BURNING OF AIR-PROPANE MIXTURES

UPSTREAM VELOCITY - FT/SEC.



D - DISTANCE FROM HOLDER TO OUTLET - IN.

Flow Associated with the V-Flame

A report (UMM-43) entitled "Resonance of a V-flame in a Parallel-walled Combustion Chamber" has been written. Preliminary copies will be distributed. This report covers all the experimental work done on the confined V-flame and relates this experimental work with the theoretical predictions for resonant flow in the combustion chamber.

Detonation

As indicated in the future program of the last progress report, detonation tests and development of the photographic system was continued. The valve assembly has been perfected. Now there are no leaks in the downstream direction, and any desired fuel-air mixture can be maintained in the test section. The reservoir pressure can now be set and controlled. This is important because, as proven during this period, the velocity of the shock wave is very sensitive to the pressure ratio between the reservoir and test section gases.

A new film pack was fabricated which exposed three feet of strip film each time the spark was triggered. This helped to locate the shock. A new trip arrangement was installed. It was found that the present electronic photoelectric system was not reproducible with any degree of accuracy. The new trigger arrangement is similar to the one developed at Cornell University by Kantrowitz. It consists merely of a copper tube which parallels the test section of the shock tube. As a main shock moves down the test section and passes by a pressure pick-up located in the wall of the test section, a secondary shock wave is formed in the copper tube. This secondary shock is then used to trip a mechanical contact. When the mechanical contact is hit by the secondary shock wave, an electrical circuit is completed which triggers the spark source.

A series of shadowgraph pictures were taken at Mach numbers from 2 to 4 with this new trip arrangement. The first pictures were taken at the downstream end of the test section where the test section gases had expanded to atmospheric pressure. The typical stationary exit shock was formed. This shock was then moved upstream into the test section. A rod was inserted normal to the flow in the test section. An oblique shock was formed off this rod in the supersonic portion of the flow behind the moving shock wave. This flow is supersonic relative to the holder but subsonic relative to the shock front (ref. EMG-14).

The shadowgraphs of the shock waves taken outside of the test section were compared to those taken inside the test section. Those taken through the plexi-glass windows of the test section were very difficult to detect even though they were stationary shock waves.

Small bits of tracing paper were then placed within the test section at uniform intervals to help locate the moving shock wave. These bits of paper were set into motion by the supersonic stream after passage of the moving shock wave and appeared as blurred lines in the shadowgraph pictures. The Mach number of the flow behind the shock wave, computed from the angle formed with the rod, was about 1.7. The theoretical Mach number of this same portion of flow was 1.8. Experimental and theoretical values, therefore, showed close agreement.

The theoretical Mach number of the moving shock wave relative to the undisturbed gas ahead of it was 2.95. Since the bits of paper traveling at a Mach number of 1.7 were blurred in the shadowgraphs mentioned above, it was believed that the moving shock wave, traveling faster than the gas behind it would also be blurred and impossible to detect in the shadowgraph pictures. This proved to be the case.

Conclusions from these pictures are as follows: (1) it will be necessary to replace the plexiglass windows, which are subject to abrasion, by optically flat glass so that the thin shock waves produced in the shock tube can be detected; (2) the spark source will be made to operate more quickly so that the moving shock wave traveling down the test section can be stopped.

Blowdown System

Heat Exchanger - Several heating runs have been made and data obtained on the temperature of the exit air versus time of run (see Figure 17). It will be noticed that the temperatures obtained are not up to the 1000°F required. Due to the correction of several operating difficulties, higher exit temperatures and mass flows are expected.

Data for Run I were taken before the heat exchanger bed had been packed completely with grog. Considerable channeling of the flow resulted with poorer heat transfer from the bed to the air flow, giving a continual decrease of exit air temperature with time. Data for succeeding runs were taken after the bed was completely filled, showing the effects of reduced channeling and a better heat transfer from the grog to the air.

Initially, trouble was encountered with the propane heating system. Fuel-air mixtures were injected, with the fuel flow entraining air for combustion. The bed resistance put a limit on the amounts of propane that could be added with the result that bed temperatures stabilized at much lower temperatures than desired. This problem was corrected by forcing the fuel-air mixture through the packed bed with air directly from the storage tanks.

Channeling of the air along the upper surface of the heat exchanger posed a second problem. During the heating cycle, the upper surface of the heat exchanger expanded considerably more than the lower surface with the result that the heat exchanger bowed upward 3 or 4 inches at the middle, remaining supported only at the ends. The opposite occurred during the cooling cycle, the pipe bowing upwards at the ends approximately 4 inches. It was necessary to add a water cooling system to keep the temperature of the exchanger shell uniform during the heating and cooling runs. To prevent excessive channeling, the grog was removed and graded so that only large particles 1/2 inch and above are packed in the bed.

Mass flow data are estimated only, since accurate flow measuring instruments were not on hand at the time of runs. The estimates are based upon total reservoir pressure drop during a given time interval at an estimated reservoir temperature.

A test section to check the effect of mixture temperature on blowoff velocities has also been built and is being calibrated (see Figure 18). It is hoped that some definite flame holding trends which are a function of mixture temperature for a given mixture and system can be observed.

Hypersonic Flow Studies - Work is progressing on a Mach 6 nozzle designed for low mass flows. Drawings have been made and materials ordered. It is planned that the nozzle will be incorporated at some point in the blowdown system so that high pressure air may be used.

- 1 - HEAT EXCHANGER
- 2 - BLOW-OUT DIAPHRAGM
- 3 - PROPANE HEATING LINE
- 4 - IGNITION
- 5 - PRESSURE CONTROL VALVE
- 6 - REDUCING VALVE
- 7 - WATER COOLING TRAY
- 8 - SYSTEM ON-OFF VALVE
- 9 - TEST SECTION
- 10 - AIR STORAGE TANKS
- 11 - AIR COMPRESSORS

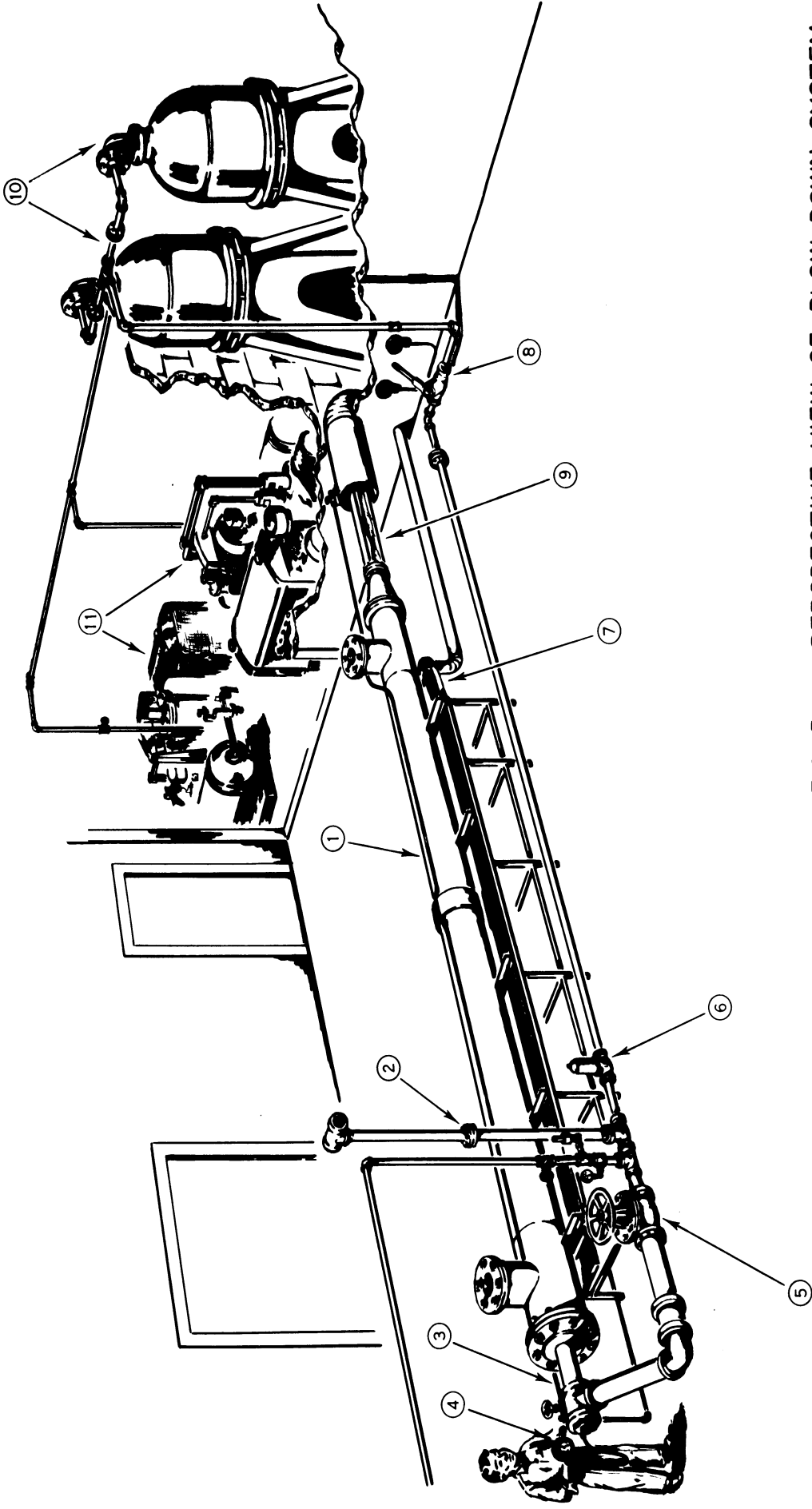
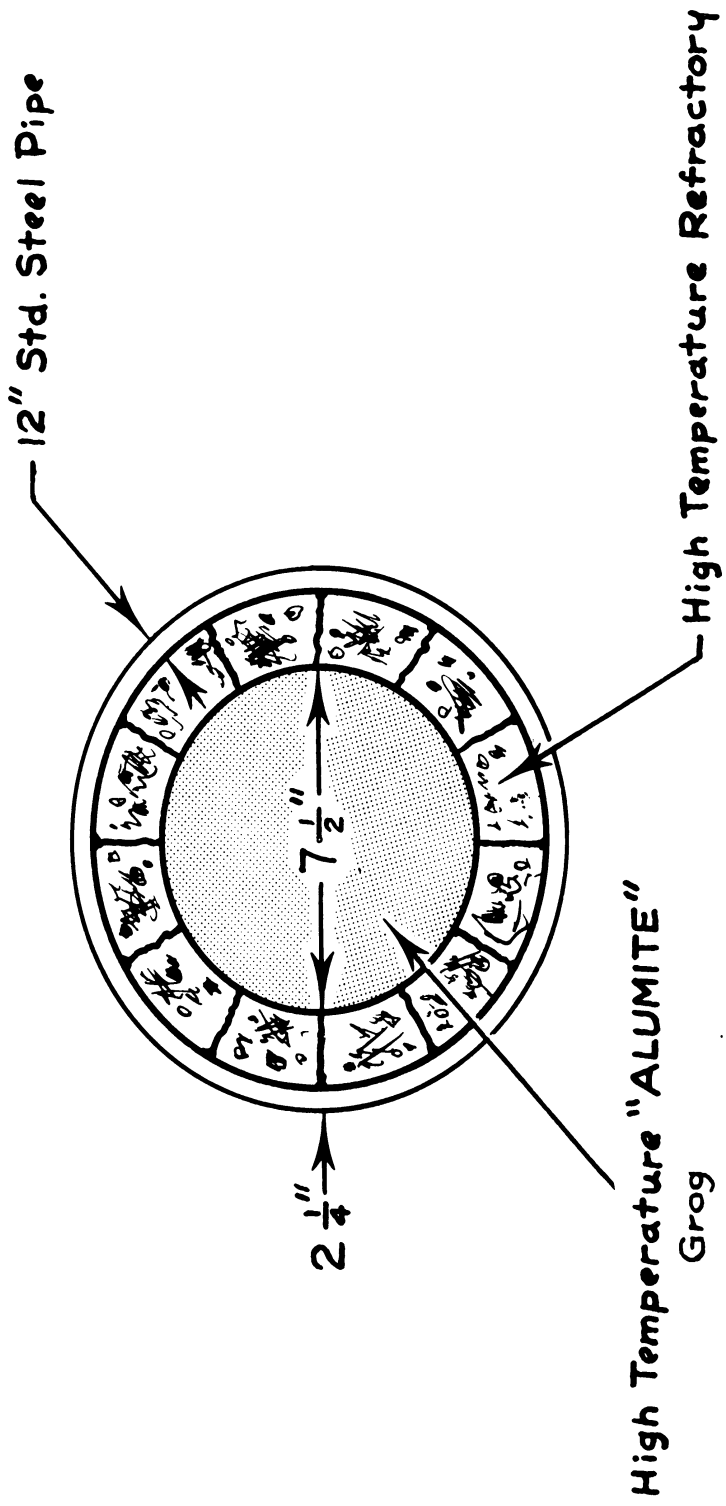


FIG. 15 - PERSPECTIVE VIEW OF BLOW-DOWN SYSTEM

UMR-37



CROSS-SECTION OF HEAT EXCHANGER

FIG. 16

UMR-37

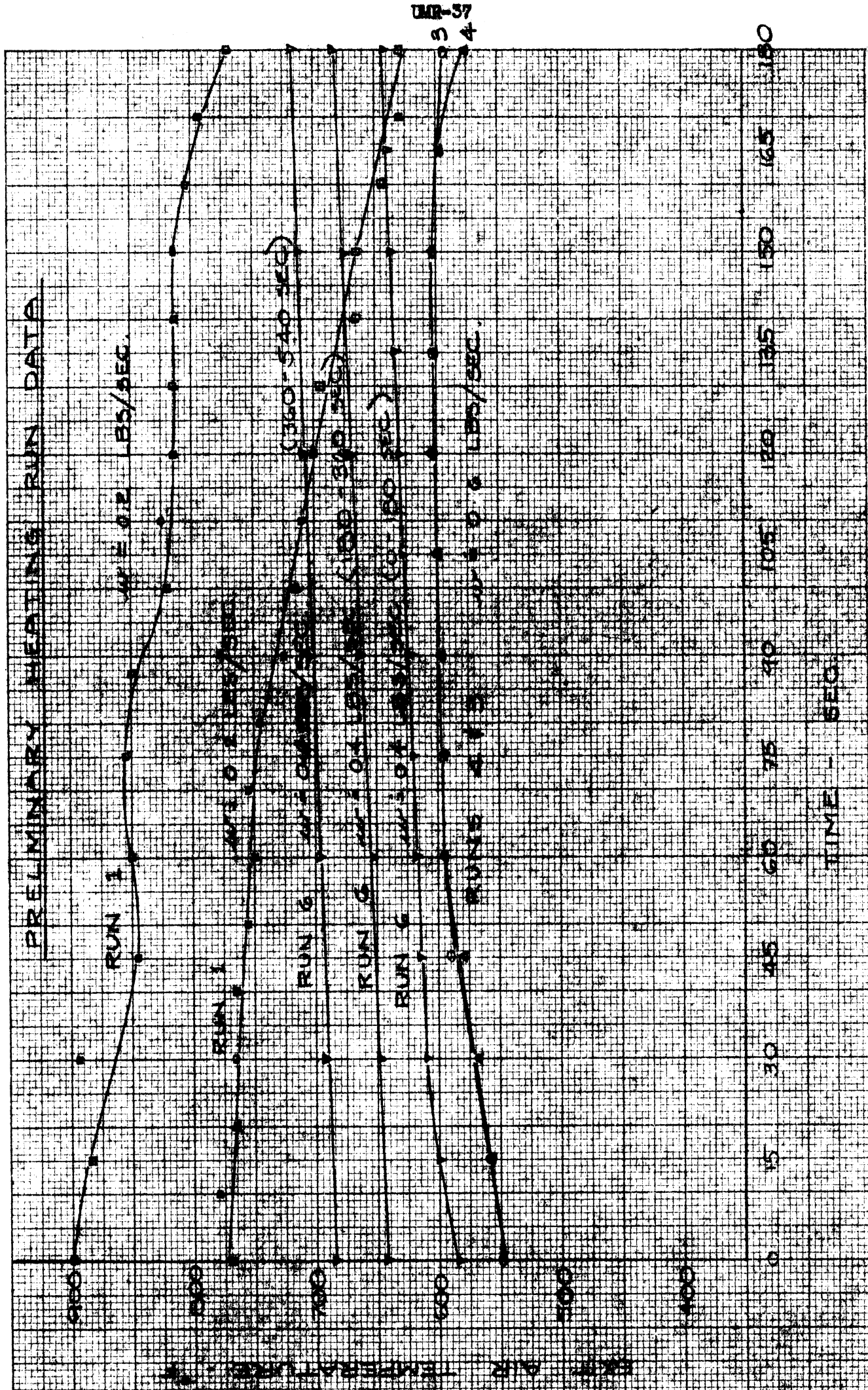
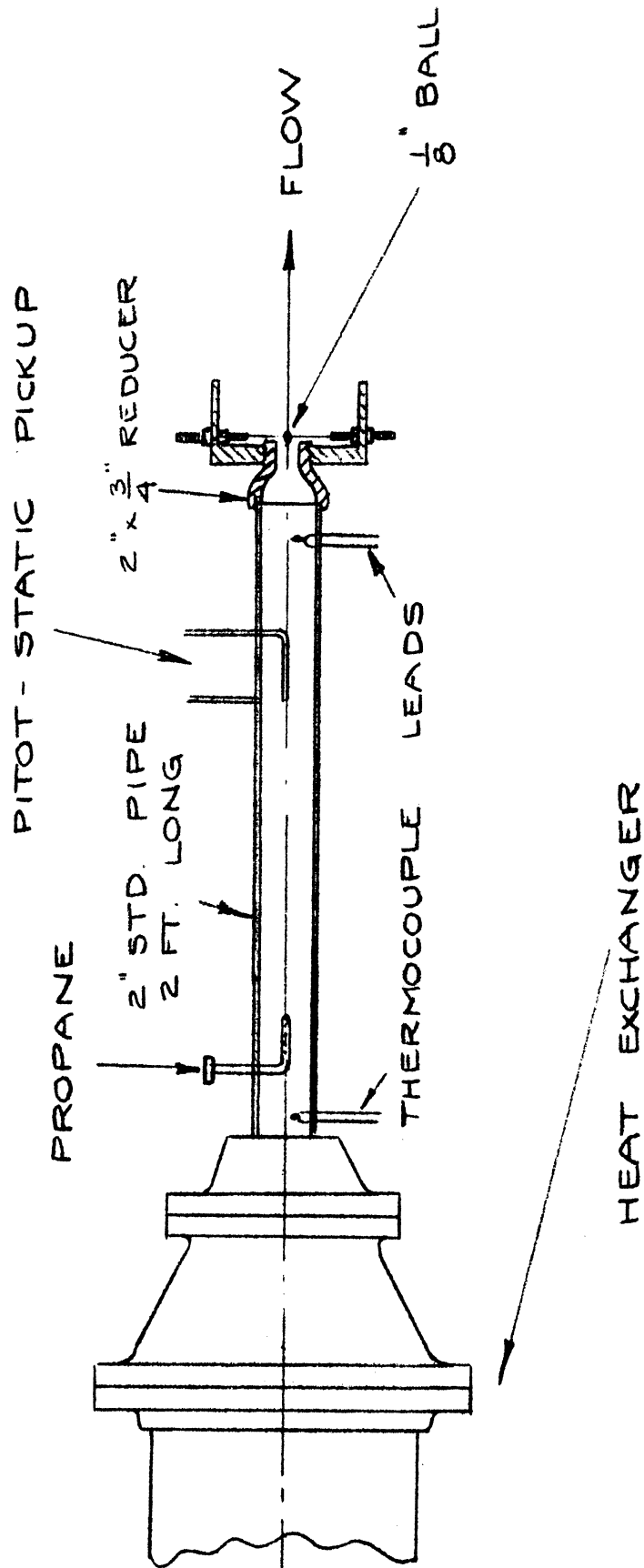


Figure 17



BLOWOFF VELOCITY
TEST SECTION

Figure 18

Experimental Techniques and Instrumentation

Interferometer - The preliminary design of the light source assembly was completed, and detail design was begun. The main case detail design was completed and an order placed for fabrication. Preliminary layouts and calculations for the projection box were started.

The optical flats (plane mirrors) were received during this period from Optron Laboratory and are being held in the original packing until the interferometer is ready for assembly. Delivery of the plate frames and miscellaneous small parts was also made during this period. Acceptance is pending inspection.

Further study of the probable problems involved in the application of the interferometer to combustion studies is being made. Methods of reduction of interferogram data are also being studied.

Shadowgraph Equipment - Construction of a photoflash unit for the laboratory has been completed. This unit uses a glow discharge lamp as a light source. The maximum input to the lamp is about 72 watt seconds and is supplied by a 16 mfd. condenser charged to a direct current potential of 3000 volts. The duration of the flash has not been measured, but durations of approximately 100 microseconds and less can be expected with this type of equipment. Triggering of the lamp is accomplished by use of a third electrode into which a high voltage pulse is introduced by means of a spark coil.

The photoflash unit gives exposure times for photography that are between those produced by a spark gap and a mechanical shutter and in this way complements them.

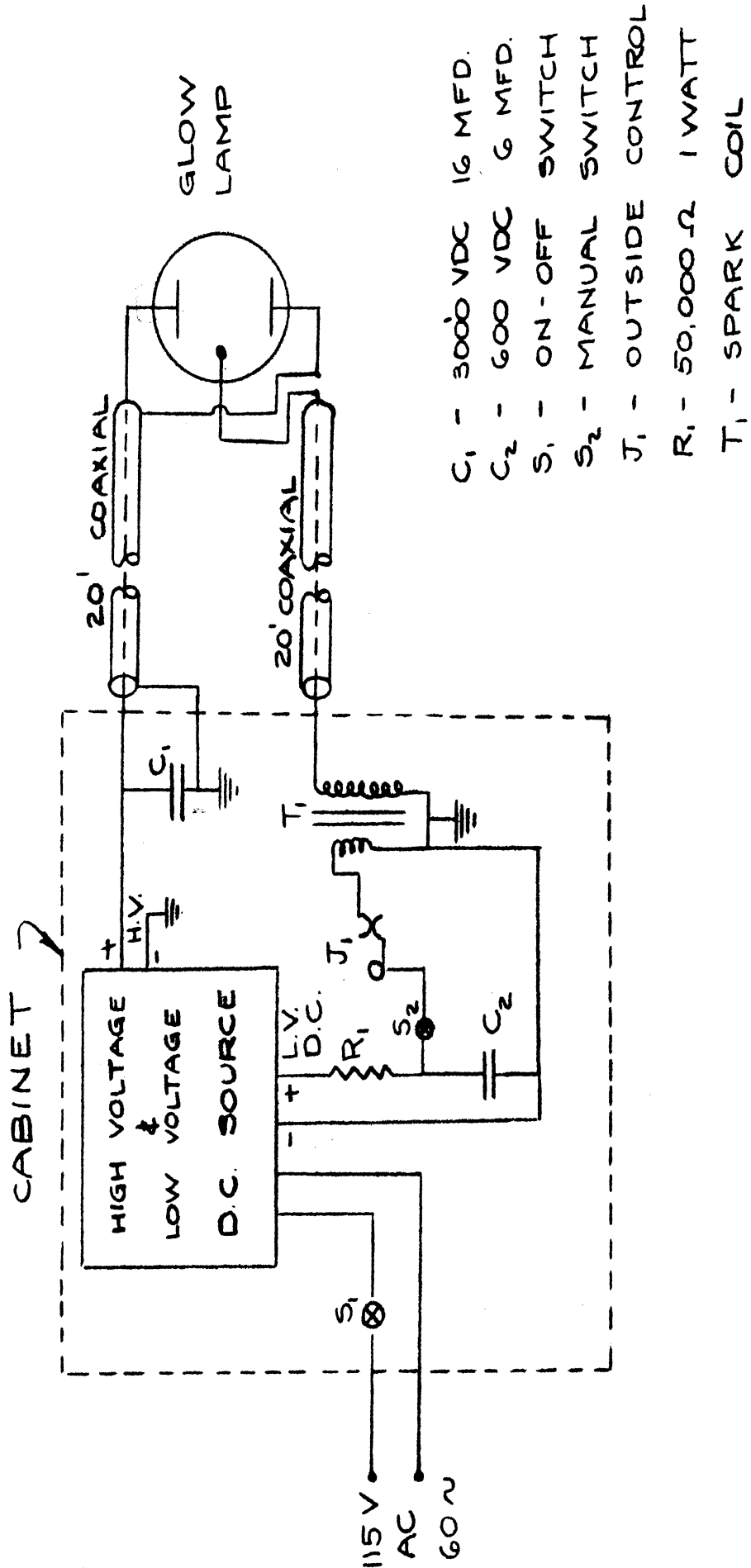
One of the shortcomings of the glow discharge lamp, for certain purposes anyway, is that it does not provide a point source of light and hence is of little use in making shadowgraphs.

The apparatus has been used for photographing fuel sprays and has worked quite well in this application. Numerous other applications are planned for this apparatus.

A circuit diagram of the photoflash unit is included in Figure 19.

UMR-37

Figure 19



- C₁ - 3000 VDC 16 MFD.
- C₂ - 600 VDC 6 MFD.
- S₁ - ON-OFF SWITCH
- S₂ - MANUAL SWITCH
- J₁ - OUTSIDE CONTROL
- R₁ - 50,000 Ω 1 WATT
- T₁ - SPARK COIL

SCHEMATIC OF PHOTOFLASH UNIT

H.H.H.

IV. PROGRAM PLANNED FOR PERIOD 10 (1 January to 1 March, 1950)

Blowoff Velocities of Flame Holders and Pressure and Temperature Effects on Combustion

It is planned to obtain blowoff data for 1/16", 3/32", 1/8", and 0.19" diameter spherical flame holders at atmospheric pressure and at a fuel-air ratio of 0.080 for the following jet diameters: 1/4", 3/8", 7/16", 1/2" and 5/8". It is further planned to obtain shadowgraph pictures of flames in the various jet sizes. It is hoped that these data will provide some correlation involving jet diameters for the different spherical flame holders used.

Combustion Chamber Design

Four-inch Combustion Chamber - The study of rough burning and combustion efficiency will be continued with emphasis placed upon the relative position of injection nozzle to flame holder. The blocking effect of various funnel-type flame holders will be tested first.

High Intensity Combustion - Further study of the effects of radiation on the combustion process will be made. Liners of various porosities, roughnesses, and melting points will be tested in an attempt to determine the important variables affecting combustion.

Flow Associated with the V-flame

Work will be continued on the resonant V-flame.

Detonation

New test section windows will be installed and alterations necessary for a faster spark source will be developed. Detonation studies will be continued.

Blowdown Equipment

Heat Exchanger - Combustion tests will be made in an attempt to find the effect of mixture temperature upon the flame holding ability of a given system at atmospheric pressure.

Hypersonic Flow Studies - The construction of the Mach 6 nozzle will be continued.

Experimental Techniques and Instrumentation

Interferometer - Design work on the interferometer and interferometer installation will be continued.

Shadowgraph Equipment - Plans are underway to improve the spark gap technique to give exposure times of approximately 0.1 microsecond.

ACTIVITIES VISITED

Activities Visited

Massillon Refractories Company
Massillon, Ohio

AMC, Wright Field
Dayton, Ohio

Subject Discussed

High Temperature
Refractories

Progress Report

BIBLIOGRAPHY

- 1a) Progress Report No. 8 -- UMR-36 -- University of Michigan
AAF Contract W33-038 ac-21100 - Page 33
- 2a) Ibid. - Page 9
- 3a) Ibid. - Page 8, Figure 2
- 4a) Ibid. - Pages 15, 16, 17, and 18; Figures 8, 9, 10, and 11
- 5a) Ibid. - Pages 19 and 20; Figures 12 and 13
- 6a) Ibid. - Page 21; Figure 14
- 7) Ibid. - Pages 15, 16, 17, and 18

DISTRIBUTION

7 Black and White Copies

1 Tracing (Opaque Ribbon)

TO: Commanding General
Air Materiel Command
Wright-Patterson Air Force Base
Dayton, Ohio